Electronic structure of some Heusler alloys based on aluminum and tin

A. Ślebarski, A. Wrona, and T. Zawada
Institute of Physics, University of Silesia, 40-007 Katowice, Poland

A. Jezierski
Institute of Molecular Physics, Polish Academy of Sciences, 60-179 Poznań, Poland

A. Zygmunt
Institute for Low Temperature and Structure Research, Polish Academy of Sciences, 50-950 Wrocław, Poland

K. Szot
Institute für Festkörperforschung, Forschungszentrum Jülich GmbH, 52425 Jülich, Germany

S. Chiuzbaian and M. Neumann
Universität Osnabrück, Fachbereich Physik, D-49069 Osnabrück, Germany
(Received 25 July 2001; revised manuscript received 28 November 2001; published 1 April 2002)

We report on the magnetic properties and electronic structure of Cu_2CrAl, and Fe_xTiSn, $Fe_{2-x}Ni_xTiSn$, and $Fe_{2-x}Co_xTiSn$ cubic solid solutions. The analysis of the magnetic susceptibility $\chi(T)$, electrical resistivity $\rho(T)$, and lattice thermal expansion $a(T)$ data allowed us to find the existence of a thermodynamic phase transition in all samples at ~ 240 K. The observed anomalies at ~ 240 K provide evidence of an isostructural phase transition which could be created by a large strain due to a small size of grains. Fe_2TiSn was observed by high-resolution electron microscopy to be composed of nanosized solid solution grains of the order of 100 nm. We discuss the superparamagnetic behavior in these alloys which results from an atomic disorder.

DOI: 10.1103/PhysRevB.65.144430 PACS number(s): 75.20.Hr, 71.20.Be, 71.27.+a, 33.60.Fy

I. INTRODUCTION

Heusler alloys[1,2] are ternary $L2_1$ compounds of the form X_2YZ, where X and Y are two different transition metals and Z is a nonmagnetic metal or a nonmetallic element. Most of these compounds are magnetically ordered; their magnetism is due to one or more $3d$ elements occupying the X or Y sites, or both. The origin of the ferromagnetism and the problem of the local magnetic moment—that is, localized behavior in some aspects of itinerant d electrons—constitute a challenging problem for the Heusler alloys. In Heusler alloys of the X_2MnZ type the magnetic moment of Mn atoms is about $4\mu_B$; it was reported in Refs. 3–6 to be independent of the nature of the X element and the Z element, and behaves like localized Mn moments in an insulator.[7] The magnetic behavior of the Co_2YZ or Fe_2YZ alloys contrast sharply with that of most of the Mn Heusler alloys; the itinerant character of the $3d$ electrons and the strong dependence of the magnetic moment μ of Co or Fe atoms on the partner elements Y and Z are almost always observed. Most of these compounds are found to exhibit some degree of atomic disorder, which is exposed in their electronic properties.

Recently, we have been engaged in a systematic study of the cubic $L2_1$-type intermetallic compound Fe_2TiSn, the magnetic and electrical transport properties of which are in strong correlation with the local environment of Fe atoms.[8,9] Fe_2TiSn has a number of properties that make it of current interest. Within the LMTO (localized muffin tin orbital) approximation, electronic structure calculations indicated that Fe_2TiSn should be a nonmagnetic semimetal with a pseudogap in the density of states (DOS) at the Fermi level. The calculations predicted that the stoichiometric compound has no magnetic transition, whereas the disordered alloy in which Fe and Ti are intermixed should be magnetically ordered,[10] in agreement with observation.[8] An anomalous behavior of the specific heat was also observed for Fe_2TiSn,[8] where the electronic component was reported to have a broad peak at 1 K, yielding evidence of the formation of ferromagnetic correlations and heavy quasiparticles with an effective mass of ~ 40 times the free-electron mass.

In order to better understand the influence of the local environment on the electronic structure and magnetic properties of Fe_2TiSn-type alloys we have investigated Cu_2CrAl. In this paper, we report electrical transport, magnetic, and x-ray photoemission (XPS) measurements on Cu_2CrAl, which heretofore has not been investigated in detail,[7] to our knowledge, as well as *ab initio* electronic structure calculations using the LMTO method. These measurements yield evidence of the weak magnetic ground state and a ''Kondo-like'' behavior, while the electronic structure calculations predict the nonmagnetic ground state of the Cu_2CrAl compound. However, the change in the DOS at the Fermi level of the Cu_2CrAl due to the local environment of Cr atoms leads to the magnetic ground state.

We also discuss an abnormal change of the slope in the experimental lattice parameters $a(T)$ visible at ~ 240 K for Fe_2TiSn, $Fe_{2-x}M_xTiSn$, where M = Ni or Co, and Cu_2CrAl. The observed anomalies in all examples provide evidence of an isostructural phase transition which could be created by an atomic disorder. This transition appears to be magnetic in nature, as evidenced by a small hump at ~ 240 K in the $\chi(T)$ curves.

Also reported herein are the results of an investigation of the electronic structure and crystallographic properties of $Fe_{2-x}Ni_xTiSn$, $Fe_{2-x}Co_xTiSn$, and Fe_xTiSn alloys. Such studies are used to determine the density of states of the alloys, and, more interestingly, the contribution of the constituent elements to the valence bands. We also discuss the strongly hybridized *d*-electron states which form a peak located in the DOS at the Fermi level, and its influence on the stability of the crystalline structure of the alloys.

II. EXPERIMENT

Polycrystalline samples of $Fe_{2-x}Ni_xTiSn$, $Fe_{2-x}Co_xTiSn$, Fe_xTiSn, and Cu_2CrAl alloys were arc melted on a water-cooled copper hearth in a high-purity argon atmosphere with a Zr getter. X-ray-diffraction analysis revealed that the alloys consisted of a single phase with a cubic $L2_1$-type Heusler structure. The structure of the samples was studied between 10 and 300 K by x-ray diffraction, with Cu $K\alpha$ radiation, using a Siemens D-5000 diffractometer. The dc magnetization was measured using a commercial superconducting quantum interference device magnetometer from 1.8 to 400 K in magnetic fields up to 5 T. Electrical resistivity measurements were performed between 4.2 and 300 K, using a standard four-wire ac method. The XPS spectra were obtained with monochromatized Al K_α radiation at room temperature with a total energy resolution of about 0.3 eV using a PHI 5700 ESCA spectrometer. The electronic densities of states were calculated using a spin-polarized self-consistent tight-binding linear-muffin-tin-orbital method[11] within the framework of the local-spin-density approximation. Further insight was gained with a comprehensive transmission electron microscopy (TEM) study. Conventional TEM in support of the high resolution work was done in a JEM 2000FX microscope operated at 200 kV analytical data collection and selected area electron-diffraction (SAED) patterns were recorded in a CM 200 FEG microscope operating in the nanoprobe mode.

III. RESULTS AND DISCUSSION

A. $Fe_{2-x}M_xTiSn$, where M=Ni, Co

The resistivity and magnetic susceptibility data presented in Ref. 9 provide further evidence of the Kondo-lattice behavior of Fe_2TiSn. The resistivity $\rho(T)$ of Fe_2TiSn and $Fe_{2-x}Ni_xTiSn$ alloys varies as $\ln T$ below ~ 50 K, while the $\rho(T)$ curves are quite different and typical of spin fluctuations for $Fe_{2-x}Co_xTiSn$.[9] In the picture of a Kondo-lattice description, the weak ferromagnetism observed for Fe_2TiSn was discussed in Ref. 9 as a result of local magnetic moments of Fe that are not Kondo compensated. In view of band-structure calculations and resistivity $\rho(T)$ and magnetic susceptibility $\chi(T)$ data, we have identified Fe_2TiSn as a weakly ferromagnetic Kondo system with a semiconducting gap that, however, is strongly reduced by the local environment. A similar feature in the electronic structure and a semiconductor like resistance anomaly were observed in FeSi, which has been classified[12] as a unique *d*-electron system that belongs to the family of Kondo insulators. The spin-polarized band calculation for Fe_2TiSn with a cubically ordered $L2_1$-type structure showed that the system is paramagnetic.[8] The magnetic moment localized on Fe atoms depends strongly on the local environment, and its value changes from $0\mu_B$ to $2.7\mu_B$ depending on the degree of atomic disorder. In Fig. 1 we present numerical calculations of the electronic DOS of $Fe_{2-x}Ni_xTiSn$ and $Fe_{2-x}Co_xTiSn$. Also shown in the figure, for comparison, are the XPS valence-band spectra. The density of states was convoluted by Lorentzians with a half-width of 0.4 eV to account for the instrumental resolution. The partial DOS's were multiplied by the corresponding cross sections.[13] A background, calculated by means of a Tougaard algorithm,[14] was subtracted from the XPS data. The spectra were measured at room temperature, i.e., above the Curie temperature (or the temperature of the formation of superparamagnetic clusters[9]); therefore, to obtain a better agreement between the experimental and calculated bands, in Fig. 1 we compare the XPS valence-band spectra with the calculated one for the paramagnetic alloy. The bands extend from the Fermi energy to a binding energy of about 10 eV, and are characterized by a major peak located at about 2 eV due to Fe, Ti, and *M*-metal *d* states. A weak peak is located at about 8 eV due to Sn *s* states. The calculations agree well with the XPS valence-band spectra. The DOS values at ϵ_F are strongly dependent on the Ni or

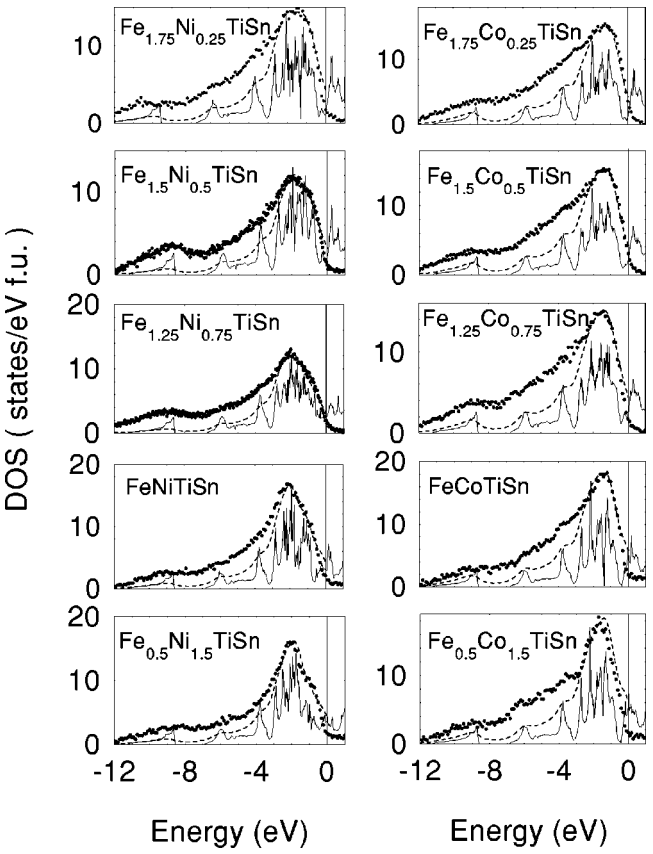

FIG. 1. The total DOS calculated for the paramagnetic $Fe_{2-x}M_xTiSn$ alloys, where M=Ni or Co (thin curve), convoluted by Lorentzians of half-width 0.4 eV, taking into account the proper cross sections for bands with different *l* symmetry (dashed line), are compared to the measured XPS valence-band data corrected for background (points).

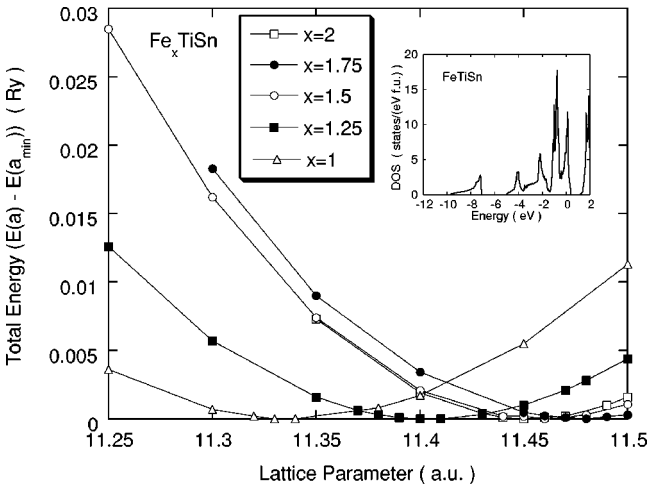

FIG. 2. The total energy as a function of the Wigner-Seitz radius r_{WS} (lattice parameter a) for Fe_xTiSn. The r_{WS} values obtained experimentally for the polycrystalline samples are $\sim$11.48 for $Fe_{1.9}TiSn$ and $Fe_{1.8}TiSn$, and $\sim$11.49 for $Fe_{1.6}TiSn$. Inset: numerical calculations of the DOS of the cubic FeTiSn (space group $Fm3m$).

Co concentration. The spin-polarized tight-binding LMTO calculations indicate that the chemical disorder gives rise to the magnetic moment on Fe atoms.

Using the *ab initio* LMTO method, we try to determine whether the disordered alloy Fe_xTiSn is a semiconductor or metal. The solid solution with the $L2_1$ structure only forms in Fe_xTiSn for $x \geqslant 1.6$. In the band calculations we assume that one fcc sublattice is occupied by iron atoms, and we change the number of Fe only in the second fcc sublattice. This procedure leads to the lowest energy at the minimum. Spin-polarized band calculations showed that all Fe_xTiSn alloys are paramagnetic. The total DOS's were obtained using the experimental lattice parameters, and the lattice parameters obtained by a minimization of the total energy with respect to the volume. In both cases the total DOS's are very similar.

Shown in Fig. 2 is a plot of the calculated total energy, relative to its minimum value vs the lattice parameter a for Fe_xTiSn. Our theoretical results indicate that up to $x=1.5$ the lattice parameters at the minimum of the total energy are very similar to that obtained experimentally by x-ray diffraction on the Fe_xTiSn samples. However, for $Fe_{1.25}TiSn$ and FeTiSn the calculations predict lattice parameters which seem to be unreliable. Thus we conclude that the $Fe_{1.25}TiSn$ and FeTiSn alloys do not crystallize in the cubic structure (or cannot be obtained as a single phase). As shown in Fig. 3 and in the inset of Fig. 2, vacancies in the Fe sites reduce the pseudogap at the Fermi level and, at ϵ_F create, a narrow d-type peak in the Fe DOS. The intensity of this peak increases with decreasing x (i.e., with an increasing number of vacancies), and is obtained to be drastically large for the hypothetical compound FeTiSn.

Shown in Fig. 4 are plots of the electrical resistivity ρ vs T for Fe_xTiSn, where $x \geqslant 1.4$. In particular, the $\rho(T)$ curves show very similar behaviors at $T>100$ K, while at $T=0$ the value of the residual resistivity ρ_0 decreases with the change in the number of vacancies created on the Fe sites. As shown

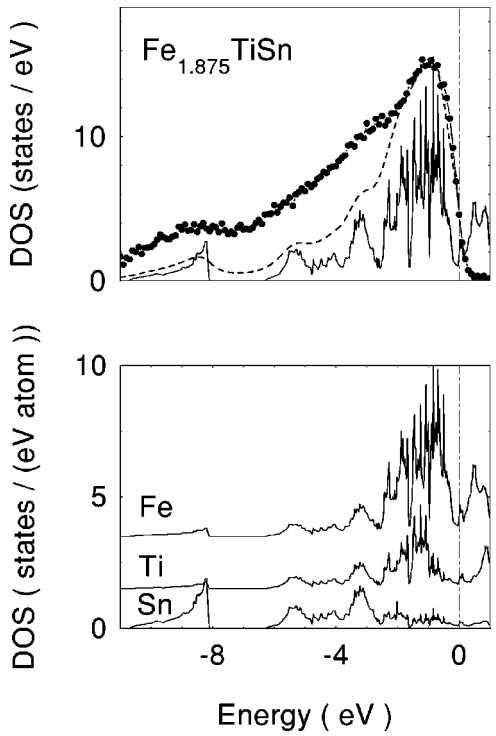

FIG. 3. The total DOS calculated for the paramagnetic $Fe_{1.875}TiSn$ (thin curve) and the calculated XPS valence-band spectra using the same procedure given in description of Fig. 1 (dashed line), are compared to the measured XPS valence-band data corrected for background (points). The partial DOS curves for Fe, Ti, and Sn are plotted below.

in Fig. 4, the $\rho(T)$ curves of Fe_xTiSn are typical of d-type metals, while the $\rho(T)$ curves of $Fe_{1.9}TiSn$ and $Fe_{1.8}TiSn$ alloys vary, as $\ln T$ below $\sim$10 K. The resistivity data presented in Fig. 4 provides further support for the band-structure calculations, which exhibit a d-type peak in the DOS located at ϵ_F, and also for Kondo-lattice behavior in

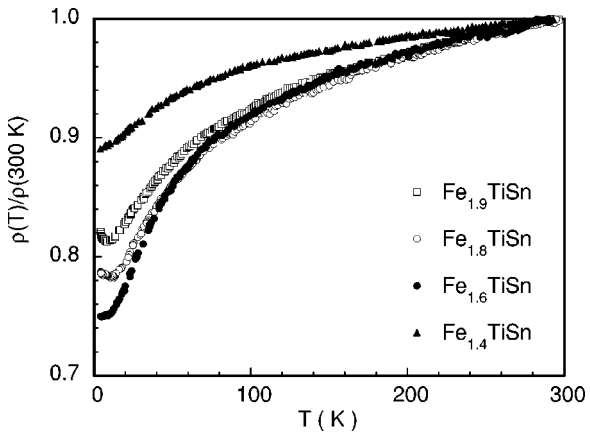

FIG. 4. Reduced electrical resistivity $\rho(T)/\rho(300\ \mathrm{K})$ vs T for Fe_xTiSn. The large value of the residual resistivity ρ_0 results from the defected crystalline structure of $Fe_x(Vac)_{2-x}TiSn$ with the increasing number of the vacancies. The largest value of ρ_0 is measured for the two-phase sample $Fe_{1.4}TiSn$, which was not obtained as a one phase sample under 2 weeks annealing.

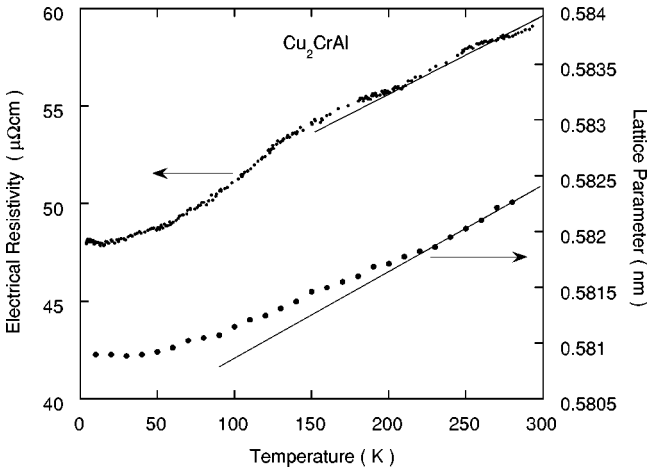

FIG. 5. Lattice parameter a and electrical resistivity ρ vs temperature for Cu_2CrAl.

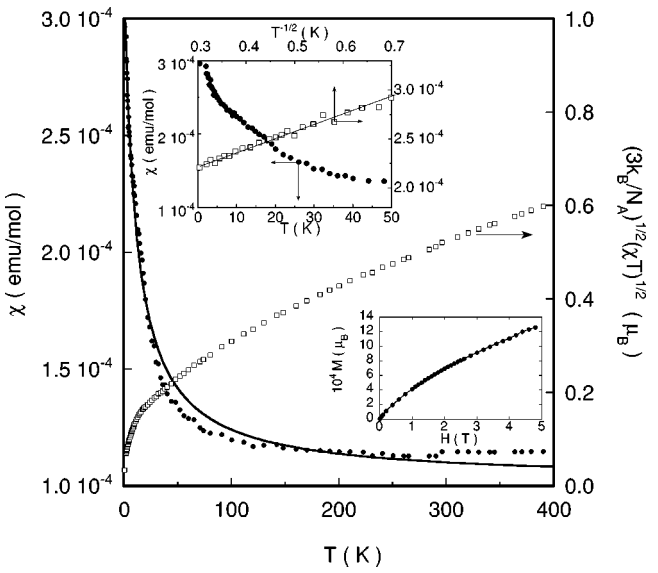

FIG. 6. Magnetic susceptibility χ and $(3k_B/N_A)^{1/2}(\chi T)^{1/2}$ vs temperature for Cu_2CrAl. The applied magnetic field was 10 kOe. The $\chi(T)$ data are fitted by the relation $\chi(T)=\chi_0+C/(T-\theta)$ (solid line). The best fit to $\chi(T)$ data yields $\chi_0=1\times10^{-4}$ emu/mol, $C=2.4\times10^{-3}$ emu K/mol, and $\theta=-11.2$ K. The inset shows the magnetization M vs the magnetic field H at $T=1.9$ K, and χ vs T and $T^{-1/2}$.

Fe_xTiSn alloys. We therefore expect that $Fe_1^{I}Fe_{x-1}^{II}(Vac)_{2-x}TiSn$ alloys, with a fully occupied Fe^{I} sublattice and a disordered occupation of the Fe^{II} sites, have magnetic moments localized on the Fe^{II} atoms, which are compensated for by Kondo-like screening.

B. Cu_2CrAl

A standard analysis of the peak positions in the powder x-ray-diffraction pattern for Cu_2CrAl showed that it crystallizes in an $L2_1$-type structure with a lattice parameter of 0.58124 nm. Displayed in Fig. 5 is a plot of the lattice parameter a determined from x-ray-diffraction measurements at various temperatures T. At ~230 K there is an abnormal change in a vs T plot which coincides with some features in $\rho(T)$, also shown in Fig. 5. The electrical resistivity ρ data plotted as ρ vs T exhibit a slight minimum at ~15 K, while for $T<15$ K ρ varies as $\ln T$, characteristic of a Kondo-type interaction.

Plots of the magnetic susceptibility χ and $(3k_B/N_A)^{1/2}\times(\chi T)^{1/2}$ vs T between 1.9 and 400 K are shown in Fig. 6. There is a sharp increase in $\chi(T)$ below ~50 K; we also note a distinct anomaly at ~10 K in the $\chi(T)$ data. The magnetic susceptibility $\chi(T)$ deviates markedly from the Curie-Weiss law signaling the onset of a magnetic ground state. $(3k_B/N_A)^{1/2}(\chi T)^{1/2}$ expresses the temperature dependence of the effective magnetic moment μ_{eff}. Since the Curie-Weiss law is followed, it saturates at temperatures higher than the temperature attributed to the crystalline electric-field splitting. However, $(\chi T)^{1/2}$, displayed in Fig. 6, does not saturate and is about $0.6\mu_B$ at 400 K, much smaller than the Cr^{3+} free-ion value of $3.87\mu_B$.

Since the magnetization M vs H up to $H=5$ T is nonlinear at $T=1.9$ K (Fig. 6), one explanation for an anomalous change in χ at ~10 K in χ vs the T plot would be superparamagnetism. The magnetic properties of Cu_2CrAl are similar to that of Fe_2TiSn,[9] or Fe_2VAl and Fe_2VGa.[15] These stoichiometric materials are nonmagnetic, while the local disorder creates a magnetic moment on Cr or Fe sites and leads to the formation of small grains. The small size of grains provides a clear criterion to form a single-domain configuration, e.g., of superparamagnetic type (it will be discussed below). Superparamagnetism would also be created in larger grains by magnetic clusters. In both cases the atomic disorder seems to be the main reason behind the anomalous behaviors observed in the magnetic-susceptibility measurements.

The susceptibility data plotted in Fig. 6 also show that χ is linear with $T^{-1/2}$ for Cu_2CrAl at $T<10$ K. Anderson[16] showed that, if spin compensation is the dominant machanism responsible for the low-temperature magnetic behavior, χ varies as $T^{-1/2}$ in the low-temperature limit; the χ vs T data in Fig. 6 is in good agreement with this theoretical prediction. Also, $(\chi T)^{1/2}$ decreases smoothly to an estimated value of $\sim0.04\mu_B$ at $T=0$. The magnetic susceptibility data shown in Fig. 6 has features similar to those in χ vs T plot for Fe_2TiSn.[9] We postulated a Kondo-lattice behavior with a partial spin compensation, which could be responsible for the susceptibility behavior in Fe_2TiSn.

Another possible source of the magnetic ground state in Cu_2CrAl would also be a volume effect. Shown in Fig. 7 is a plot of the calculated total energy, relative to its minimum value for a ferromagnetic and paramagnetic ground state, and a magnetic moment μ vs the Wigner-Seitz radius r_{WS} (or equivalently, the Wigner-Seitz volume $V_{WS}=4\pi/3r_{WS}^3$). According to the calculated μ values shown in Fig. 7, Cu_2CrAl exhibits a magnetic behavior ($\mu>0$) at the value $r_{WS}^{expt}=10.97$ which is experimentally obtained from the lattice parameter a. The calculated total energy at r_{WS}^{expt}, is however, significantly larger for the ferromagnetic ground state than the value obtained for the paramagnetic one. Thus we attribute the magnetism of Cu_2CrAl more to the atomic disorder than to the volume effect.

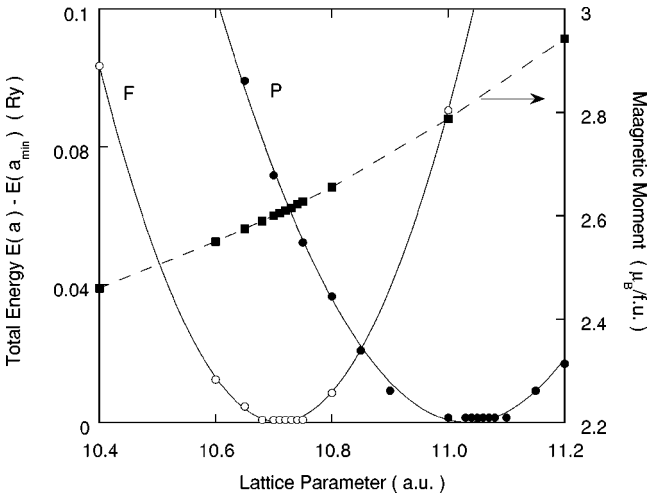

FIG. 7. Calculated magnetic moment and the total energy as a function of the Wigner-Seitz radius r_{WS} (lattice parameter a) for ferromagnetic (F) and paramagnetic (P) Cu_2CrAl. The experimental value of r_{WS} is 10.97.

The LMTO valence-band calculations for a paramagnetic Cu_2CrAl are compared to the XPS spectra in Fig. 8. The agreement between the theory and the experimental data is excellent. The spectra reveal a valence band that has a major

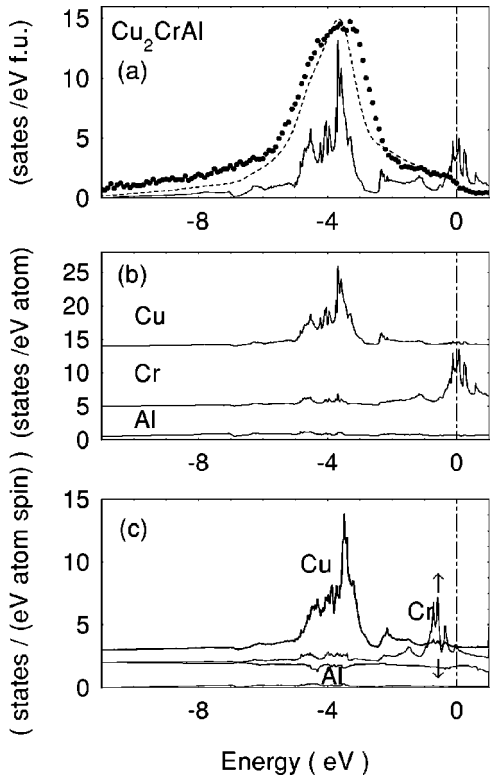

FIG. 8. Numerical calculations of the DOS of Cu_2CrAl for both spin directions (c). In (a), the total DOS calculated for the paramagnetic Cu_2CrAl (thin curve), convoluted by Lorentzians of half-width 0.4 eV, taking into account proper cross sections for bands with different l symmetry (dashed line) and measured XPS valence-band spectra corrected for the background (points). In (b), the partial DOS curves for the paramagnetic Cu_2CrAl.

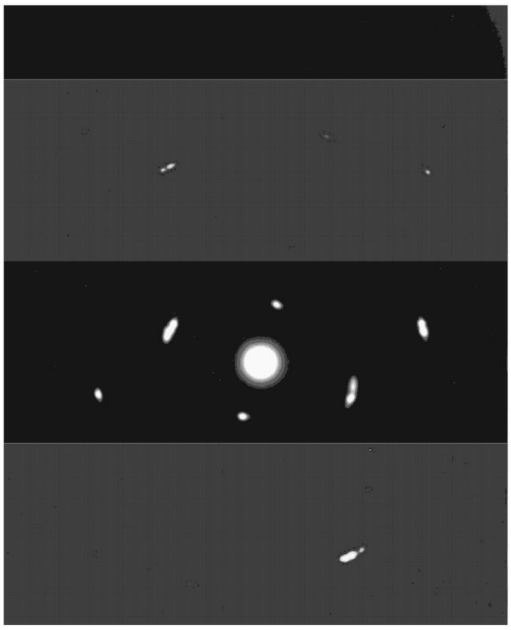

FIG. 9. SAED pattern registered for the Fe_2TiSn polycrystalline sample in one of the polycrystalline particles of ~ 100 nm in size. The composition of this grain, $Fe_{46.5}Ti_{20.5}Sn_{33}$, was checked by x-ray energy dispersive spectroscopy (XEDS).

peak due to the Cu d states located 4 eV in the band, while the Cr d states are located at the Fermi level. However, the spin-polarized band calculations performed for the ferromagnetic Cu_2CrAl showed Cr $d\uparrow$ states located 1 eV below ϵ_F, due to the Culomb interaction inside the Cr d shell.

C. Structural investigations

From the electron-diffraction analysis we obtained a very small crystallite size of a few nanometers to tens of nanometer. Figure 9 shows an electron diffraction pattern (in the selected-area electron diffraction mode) registered for Fe_2TiSn polycrystals in nanocrystalline grains about 100 nm in size. The electron-diffraction result confirms the particle crystallinity with different lattice parameters due to the local atomic disorder and different orientations. However, the SAED patterns of the different grains have never displayed rings typical of the amorphous state.

A more detailed analysis of the x-ray-diffraction data [Fig. 10(a)], in which the crystal structure of Fe_2TiSn was refined with the Rietveld method,[17] also revealed the presence of crystallographic disorder. The lower value of the R factor ($R_{wp}=4.9$) corresponds to the occupation of the Ti site by Fe in every fifth unit cell. However, the shape of the reflections are not in good agreement with the calculations, particularly in the 2θ range of the tail of each line, which we attribute to the small size of the grains. Texturing the powdered sample on the x-ray slide could also shift the relative intensities of the diffraction peaks in a way similar to chemical disorder. Thus, to exclude this possibility, we have analyzed the x-ray-diffraction patterns obtained for two different (perpendicular) positions, one position of the powdered sample at an angle of $\alpha=0°$ and another one corresponding

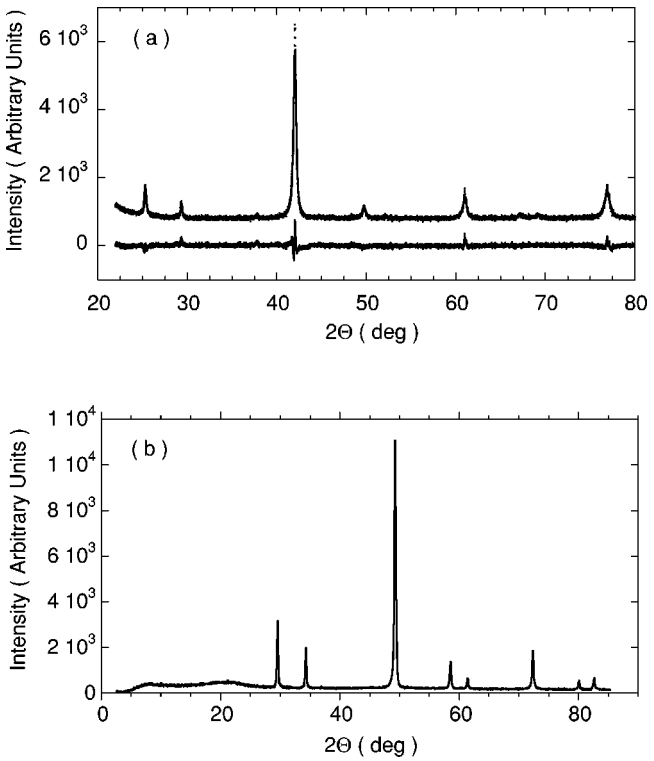

FIG. 10. (a) The observed (points) and calculated (solid line) x-ray-diffraction patterns of Fe_2TiSn. The bottom is the difference between the observed and calculated intensities after Rietveld refinement. The x-ray powder diffraction was carried out with Fe $K\alpha$ radiation. (b) X-ray-diffraction pattern of Fe_2TiSn (obtained with Cr $K\alpha$) subtracted by background.

to a rotation of $\alpha = 90°$ in the plane of the x-ray slide. It is noteworthy that both diffraction patterns of these two geometries were identical. Shown in Fig. 10(b) are x-ray-diffraction data of Fe_2TiSn obtained with background correction (the x-ray reference measurement of a glue was subtracted from the x-ray diffraction pattern) for $2.5° < 2\theta < 85°$ with monochromatized Co $K\alpha$ radiation using a STOE diffractometer. The x-ray powder diffraction pattern does not display any amorphous background at the low 2θ values (greater than the reference x-ray diffraction pattern which was subtracted). On the basis of the x-ray-diffraction data we are drawn to the same conclusion as obtained from the SAED.

The mesoscopic size of the grains provides a clear criterion to form the single-domain configuration of the superparamagneticlike materials. As mentioned above, the local disorder can lead, in Fe_2TiSn-type alloys, to superparamagnetic features. When the size of the magnetic grains enters into the nanometer scale, the particle moments rotate coherently if the thermal energy exceeds the anisotropy barrier; this magnetic behavior is described as superparamagnetism. The relaxation time of the magnetization between two states with oppositely directed spins (i.e., two easy orientations of magnetization) is given by thermal activation formula[18,19] $\tau = \tau_0 \exp(E_a/k_B T)$, where E_a is the energy barrier separating the states and τ_0 is a microscopic limiting relaxation time, usually $\approx 10^{-9}$ s. Below a "blocking" temperature T_B of order $E_a/25k_B$, fluctuations between the two states become long enough to be observable.[19] For a still lower value of T the system appears "blocked" in one of the states. If one attributes the anomalous behavior in χ vs T at ~ 10 K in Fig. 6 to the blocking at the temperature T_B, then one also expects some anomalies at the temperature $25T_B$ in $\rho(T)$, $\chi(T)$, and $a(T)$. As mentioned above, a lattice parameter a of $Fe_{2-x}Ni_xTiSn$, plotted as a vs T between 10 and 300 K, exhibits an abrupt drop relative to the calculated $a(T)$ curve[8] at ~ 240 K. In Fig. 5 exactly the same abnormal change in $a(T)$ is shown for Cu_2CrAl at ~ 230 K. This anomalous change of the lattice parameter cannot be attributed to a structural phase transition; the x-ray-diffraction patterns indicated any change of the crystal structure. The observed anomalous change of a in the a vs T plot coincides with some features in $\rho(T)$ and $\chi(T)$, and provides evidence of the superparamagnetic behaviors.

Another reason for these anomalies at ~ 240 K could be a local strain in the small grains created by defects. In each grain a local strain which results, e.g., from the atomic disorder, becomes energetically nonfavorable, if the thermal energy exceeds $k_B T_0$, where T_0 is about 240 K. The coexistence of the lattice thermal vibration can also lead to the anomalous change observed in the lattice expansion coefficient $\alpha(T)$. It is likely that both the relaxation of the magnetic domains and the strain inside the grains are significant mechanisms.

IV. CONCLUSIONS

Within the LMTO approximation electronic structure calculations indicated that Fe_2TiSn and Cu_2CrAl should be nonmagnetic materials, whereas for the disordered alloys a magnetic ground state is obtained, in agreement with observation. Both compounds and their alloys, show similar thermodynamical properties; the magnetic susceptibility $\chi(T)$, electrical resistivity $\rho(T)$, and thermal lattice expansion $a(T)$ exhibit similar anomalies at about 240 K, which can result from superparamagnetic thermal fluctuations of the magnetic nanograins. The nanosized particles are small grains with an atomic disordering, which induce magnetic moments in Fe or Cr atoms. At ~ 10 K the magnetic domains are blocked, having one orientation of the magnetic moment, which can be partially compensated for by the magnetic moments of the conduction electrons.

ACKNOWLEDGMENTS

Two of us (A.Ś. and A.W.) thank the State Committee for Scientific Research for financial support (Project No. 5PO3B 07820). One of us (A.J.) thanks the State Committee for Scientific Research for financial support (Project No. 8T11F 02716).

[1] F. Heusler, Verh. Dtsch. Phys. Ges. **5**, 219 (1903).
[2] P. J. Webster and K. R. A. Ziebeck, in *Magnetic Properties of Metals* edited by K.-H. Hellwege and O. Madelung, Landolt-Börnstein New Series, Group III, Vol. 19, Pt. c (Springer, Berlin, 1988), p. 75.
[3] P. J. Webster, J. Phys. Chem. Solids **32**, 1221 (1971).
[4] D. P. Oxley, R. S. Tebble, and K. C. Williams, J. Appl. Phys. **34**, 1362 (1963).
[5] G. B. Johnston and E. O. Hall, J. Phys. Chem. Solids **29**, 193 (1968).
[6] J. Kübler, A. R. Wiliams, and C. B. Sommers, Phys. Rev. B **28**, 1745 (1983).
[7] K. H. J. Buschow and P. G. van Engen, J. Magn. Magn. Mater. **25**, 90 (1981).
[8] A. Ślebarski, M. B. Maple, E. J. Freeman, C. Sirvent, D. Tworuszka, M. Orzechowska, A. Wrona, A. Jezierski, S. Chiuzbaian, and M. Neumann, Phys. Rev. B **62**, 3296 (2000).
[9] A. Ślebarski, M. B. Maple, A. Wrona, and A. Winiarska, Phys. Rev. B **63**, 214416 (2001).
[10] A. Jezierski and A. Ślebarski, J. Magn. Magn. Mater. **223**, 33 (2001).
[11] O. K. Andersen and O. Jepsen, Phys. Rev. Lett. **53**, 2571 (1984); O. K. Andersen, O. Jepsen, and M. Sob, in *Electronic Structure and Its Applications*, edited by M. Yussouff (Springer, Berlin, 1987), p. 2. The values of the atomic sphere radii were taken in such a way that the sum of all atomic sphere volumes was equal to the volume of the unit cell. The exchange correlation potential was taken in form proposed by von Barth and Hedin [U. von Barth and L. Hedin, J. Phys. C **5**, 1629 (1972)]; C. D. Hu and D. C. Langreth, Phys. Scr. **32**, 391 (1985).
[12] Z. Fisk, J. L. Sarrao, S. L. Cooper, P. Nyhus, G. S. Boebinger, A. Passner, and P. C. Canfield, Physica B **223-224**, 409 (1996).
[13] J. J. Yeh and I. Lindau, At. Data Nucl. Data Tables **32**, 1 (1985).
[14] S. Tougaard and P. Sigmund, Phys. Rev. B **25**, 4452 (1982).
[15] C. S. Lue, J. H. Ross, Jr., K. D. D. Rathnayaka, D. G. Naugle, S. Y. Wu, and W.-H. Li, J. Phys.: Condens. Matter **13**, 1585 (2001).
[16] P. W. Anderson, Phys. Rev. **164**, 352 (1967).
[17] R. A. Young and F. Izumi, in *The Rietveld Method*, edited by R. A. Young (Oxford University Press, Oxford, 1993), pp. 1 and 236.
[18] C. M. Hurd, Contemp. Phys. **82**, 469 (1982).
[19] J. A. Mydosh, *Spin Glasses: An Experimental Introduction* (Taylor & Francis, London, 1993).